Characterization of Mutations in the Cytochrome *b* Subunit of the bc_1 Complex of *Rhodobacter sphaeroides* That Affect the Quinone Reductase Site (Q_c)†

Beth Hacker,‡ Blanca Barquera,‡ Antony R. Crofts,§ and Robert B. Gennis*,‡

School of Chemical Sciences and School of Life Sciences, University of Illinois, Urbana, Illinois 61801

Received October 26, 1992; Revised Manuscript Received January 29, 1993

ABSTRACT: The cytochrome *b* subunit of the bc_1 complex contains two heme components, cytochrome b_L and cytochrome b_H, and is the locus of both a quinol oxidizing site (Q_o or Q_z) and a quinone reducing site (Q_i or Q_c). The quinone reductase site has been previously characterized as the site of interaction for a set of inhibitors including antimycin A, diuron, funiculosin, and HQNO. In this paper, four highly conserved residues in the cytochrome *b* subunit of *Rhodobacter sphaeroides* (A52, H217, K251, and D252) were targeted for site-directed mutagenesis. These residues were chosen as being likely to be at or near the quinone reductase site, on the basis of known locations of missense mutations in the homologous yeast subunit that confer resistance to Q_c-directed inhibitors. The site-directed mutants all exhibit a normal rate of reduction of cytochrome b_H, suggesting a fully functional quinol oxidizing site. However, each of the mutants is impaired, to varying degrees, in the rate of reoxidation of cytochrome b_H. Two mutants (H217A and D252A) are unable to grow photosynthetically, indicating a severe defect in the bc_1 complex. In both cases, the cause of the defect is the lack of reoxidation of cytochrome b_H by ubiquinone. This is the first report of mutations that selectively impair the rate of electron transfer from cytochrome b_H to the Q_c-site. This set of mutations will be useful not only for modeling the structure of the quinone reducing site but also in elucidating the catalytic mechanism of this portion of the Q-cycle.

The cytochrome bc_1 complex (ubiquinol:cytochrome *c* oxidoreductase) is a central component of electron-transport chains in mitochondria, bacteria, and chloroplasts, where the equivalent enzyme is known as the b_6f complex (Crofts, 1985; Gabellini, 1988; Hauska et al., 1988; Trumpower, 1990a). All bc_1 and b_6f complexes contain a cytochrome *b* subunit which contains two *b* heme centers, cytochrome b_H and cytochrome b_L. The complex is thought to function through a modified Q-cycle mechanism (Crofts et al., 1983; Mitchell, 1976; Trumpower, 1990b), with the low-potential cytochrome b_L accepting electrons from a quinol oxidizing site (Q_z or Q_o) close to the periplasmic side of the bacterial membrane, and the high-potential cytochrome b_H donating electrons to a quinone reductase site (Q_c, Q_r, or Q_i site) near the cytoplasmic surface. Ubiquinol is initially oxidized by the Rieske iron–sulfur center, generating a ubisemiquinone at the Q_z-site. The ubisemiquinone, in turn, reduces cytochrome b_L, which subsequently reduces cytochrome b_H near the Q_c-site. Electron transfer across the membrane from the Q_z-site to the Q_c-site provides the electrogenic arm of a proton pump, with the main contributions to the electrical work coming from both reduction and oxidation of cytochrome b_H.

In the absence of a crystallographically defined structure for the bc_1 complex, the residues contributing to the quinol oxidizing and quinone reducing sites are unknown. In modeling studies, an important element providing constraints on the structure has been the identification of residues modified in inhibitor-resistant strains. Lesions giving rise to resistance to inhibitors acting at the Q_z-site have been studied in yeast (diRago et al., 1989) and mouse mitochondria (Howell & Gilbert, 1988), and, with more detailed kinetic analysis, in *Rhodobacter capsulatus* (Atta-Asafo-Adjei & Daldal, 1991; Daldal et al., 1989; Ding et al., 1992; Robertson et al., 1990) and *Rhodobacter sphaeroides* (Yun et al., 1990). At the Q_c-site, most information has come from mitochondrial studies in yeast (diRago et al., 1986, 1990; diRago & Colson, 1988; Weber & Wolf, 1988) and mouse (Howell et al., 1987). No spontaneous inhibitor-resistant mutants have previously been mapped at the residue level in the photosynthetic bacteria. Similar studies on herbicide-resistant strains of *Rb. capsulatus* and *Rb. sphaeroides* have been an important guide in interpreting these genetic data in terms of protein structure. All herbicide resistance lesions identified at the residue level have mapped to the Q_B-site at which the herbicides are known to bind (Baciou et al., 1991; Sinning et al., 1989), and which is well-defined in the crystallographically defined structures of the bacterial reaction centers.

It is apparent from the mapping of residues in mutants resistant to the inhibitors of the bc_1 complex that the cytochrome *b* subunit contributes major structural elements to both the Q_z- and Q_c-sites. This conclusion is based on the observation that for all mutant strains showing resistance to inhibitors of the bc_1 complex, the genetic lesions have mapped to the gene encoding the cytochrome *b* subunit of the complex. The high degree of conservation of the cytochrome *b* subunit between mitochondria and bacteria makes it possible to use data from the other species as a starting point for selecting residues likely to contribute to the quinone active sites in the cytochrome *b* of *Rb. sphaeroides*.

A three-dimensional structural model of the cytochrome *b* subunit of the bc_1 complex of *Rb. sphaeroides* has been developed (Crofts et al., 1992), using secondary structural prediction, sequence alignment, conservation of residues, and structural studies using molecular engineering approaches (Yun et al., 1991b). The structural model provides a framework on which to base experiments using site-directed mutagenesis to explore the roles of specific residues in catalysis and inhibitor binding. It is likely that highly conserved residues, as well as those which confer inhibitor-resistance,

† Supported by grants from the National Institutes of Health (PHS 5RO1 GM35438 and PHS 2RO1 GM26305).

* Address correspondence to this author.
‡ School of Chemical Sciences.
§ School of Life Sciences.

0006-2960/93/0432-4403$04.00/0

play an important role in the structure and/or function of the quinol/quinone sites. In this work, site-directed mutagenesis is used to explore residues in the cytochrome *b* subunit that might contribute to the quinone reducing site (Q_c-site) of the bc_1 complex of *Rb. sphaeroides*. The residues examined are Ala52 (Gly37), His217 (His202), Lys251 (Lys228), and Asp252 (Asp229), where the numbers in parentheses are the equivalent residues in the yeast (*Saccharomyces cerevisiae*) mitochondrial cytochrome *b* sequence. These residues were chosen either on the basis of sequence alignment with residues modified in antimycin-resistant strains (G37 and K228 in yeast) (diRago & Colson, 1988) or by the location of conserved residues close to the antimycin binding domain in the putative Q_c-site (H202 and D229 in yeast) (diRago et al., 1990; diRago & Colson, 1988). The locations of the mutations are shown in Figure 1. The phenotypical consequences of these mutations were monitored by observing effects on spectra and midpoint potentials of the cytochromes, and on the kinetics of electron transfer both to and from cytochrome b_H following flash illumination. Since electron transfer from cytochrome b_H is thought to occur to either quinone or semiquinone bound at the quinone reducing site of the bc_1 complex, analysis of the mutations should help map the locations of residues which contribute to the quinone reducing site, and indicate the role of specific residues.

MATERIALS AND METHODS

Materials. All restriction endonucleases and nucleic acid modifying enzymes were obtained from New England Biolabs, Inc., or Bethesda Research Laboratories. Synthetic deoxyoligonucleotides for DNA sequencing and mutagenesis were synthesized at the Biotechnology Center of the University of Illinois on an Applied Biosystems Model 380A DNA synthesizer.

Bacteria and Plasmids. Escherichia coli strains were grown in L broth (Sambrook et al., 1989) at 37 °C. Plasmids and their derivatives were maintained in *E. coli* strains in the presence of ampicillin (75 μg/mL), kanamycin (50 μg/mL), or tetracycline (15 μg/mL). Growth medium used with strains of *Rb. sphaeroides* containing pRK415 derivatives was supplemented with 1 μg/mL tetracycline. *Rb. sphaeroides* strains were grown photosynthetically or aerobically in Sistrom's minimal medium A (Leuking et al., 1978) by vigorous shaking at 30 °C (Kiley & Kaplan, 1988; Yun et al., 1990). A Carolina Biological far-red 750 filter was used with photosynthetic *Rb. sphaeroides* cultures containing tetracycline to minimize photooxidation of the tetracycline.

Preparation of Mutant Plasmids. The site-directed mutagenesis protocol for all mutants was as described earlier (Vandeyar et al., 1988; Yun et al., 1991a). The oligonucleotides used for mutagenesis are listed in Table I. All mutations were verified by DNA sequencing.

Plasmid pMFP was constructed to aid in screening mutants. pBC9 (Yun et al., 1990) was the original plasmid used to express mutant alleles within the intact *fbc* operon. pMFP was created to facilitate the screening of mutants, and does not change the mutant cloning procedures as previously described (Yun et al., 1991a). pPST2 contains the 1.3-kb *Pst*I restriction fragment from the *fbc* operon which was used as the mutagenesis template. A *Hinc*II-cleaved Kn^R (kanamycin resistance) cartridge derived from plasmid pUC4K (Vieira & Messing, 1982) was cloned into the *Nru*I sites of a pUC9 vector containing the 1.3-kb *Pst*I fragment. The Kn^R cartridge was then cloned into the *Sph*I–*Bgl*II sites of pBC9, yielding pMFP. Replica plating of mutants on ampicillin and ampicillin–kanamycin plates greatly increased the efficiency of obtaining mutants. Mutagenesis of Ala52 used pSS4 as a template for mutagenesis because the residue is not encoded on the *Sph*I–*Bgl*II fragment of the *fbc* operon (Yun et al., 1992).

Table I: Summary of the Codon Alterations of the Mutants

mutation	nucleotide change	oligonucleotide
Ala52Val	GCC→GTC	TCGTCCTCGTCTTCTGTC
His217Ala	CAC→GCA	GCCTTCGCATCGACGGGC
Lys251Ile	AAG→ATA	ATCATCATAGACGTCTTC
Lys251Met	AAG→ATG	ATCATCATGGACGTCTTC
Asp252Ala	GAC→GCA	ATCAAGGCAGTCTTCGCC
Asp252Asn	GAC→AAT	ATCAAGAATGTCTTCGCC

Optical Redox Titrations. Chromatophores were prepared (Bowyer et al., 1979) and chemical redox titrations were performed as previously described (Dutton, 1978; Yun et al., 1991a). Data on antimycin-induced oxidation of cytochrome b_{150} were collected using redox titration protocols with the following changes. The sample was poised at E_h 200mV, and a spectrum was scanned to serve as a base line. The sample was then poised at E_h 110 mV and scanned again. The difference spectrum (110 minus 200 mV) gives the total absorbance of cytochrome b_{150}. The sample was maintained at E_h 110 mV, and titrated with aliquots of antimycin. A spectrum was scanned after each addition until saturation of the extent of antimycin-induced oxidation. A final spectrum was taken with the sample poised at E_h −20 mV, using the same base line (the spectrum at E_h 200 mV) to provide a difference spectrum showing the absorbance of total cytochrome b_H. In several cases, independent chromatophore preparations of mutants were examined, and the midpoint potentials were found to be reproducible to well within 10 mV.

Spectrophotometric Analysis of Flash-Induced Kinetics of Cytochrome b_H. The kinetic single-beam spectrophotometer used has been described elsewhere (Crofts & Wang, 1989). The kinetics of redox changes in the cytochrome components of the bc_1 complex were measured as previously described (Crofts et al., 1983; Meinhardt & Crofts, 1983; Yun et al., 1991a).

RESULTS AND DISCUSSION

Site-Directed Mutagenesis. Site-directed mutagenesis was performed using the oligonucleotides listed in Table I. The following mutations were constructed and studied in this work (see Figure 1):Ala52 to Val (A52V); His217 to Ala (H217A); Lys251 to Ile and Met (K251I, K251M); and Asp252 to Ala and Asn (D252A, D252N). The function of each of these mutant–bc_1 complexes was tested by expressing the *fbc* alleles in a strain of *Rb. sphaeroides* (BC17) from which the wild-type chromosomal *fbc* operon was deleted (Yun et al., 1990). All strains are able to grow under aerobic and semiaerobic conditions. All of the mutant *fbc*B plasmids, with the exception of H217A and D251A, confer on strain BC17 the ability to grow photosynthetically. When strains were grown under semiaerobic conditions, synthesis of the photosynthetic apparatus was induced by subjecting the cells to lowered oxygen tension. Under these conditions, H217A growth is measurably slower than that of the other mutants, and this strain incorporates the smallest amount of photosynthetic pigments as determined by bacteriochlorophyll assay. Chromatophores prepared from the mutants were used to evaluate the optical, electrochemical, and kinetic properties of the bc_1 mutants.

Midpoint Potentials of the Cytochrome Centers. Table II presents some characteristics of the bc_1 mutants. Assembly

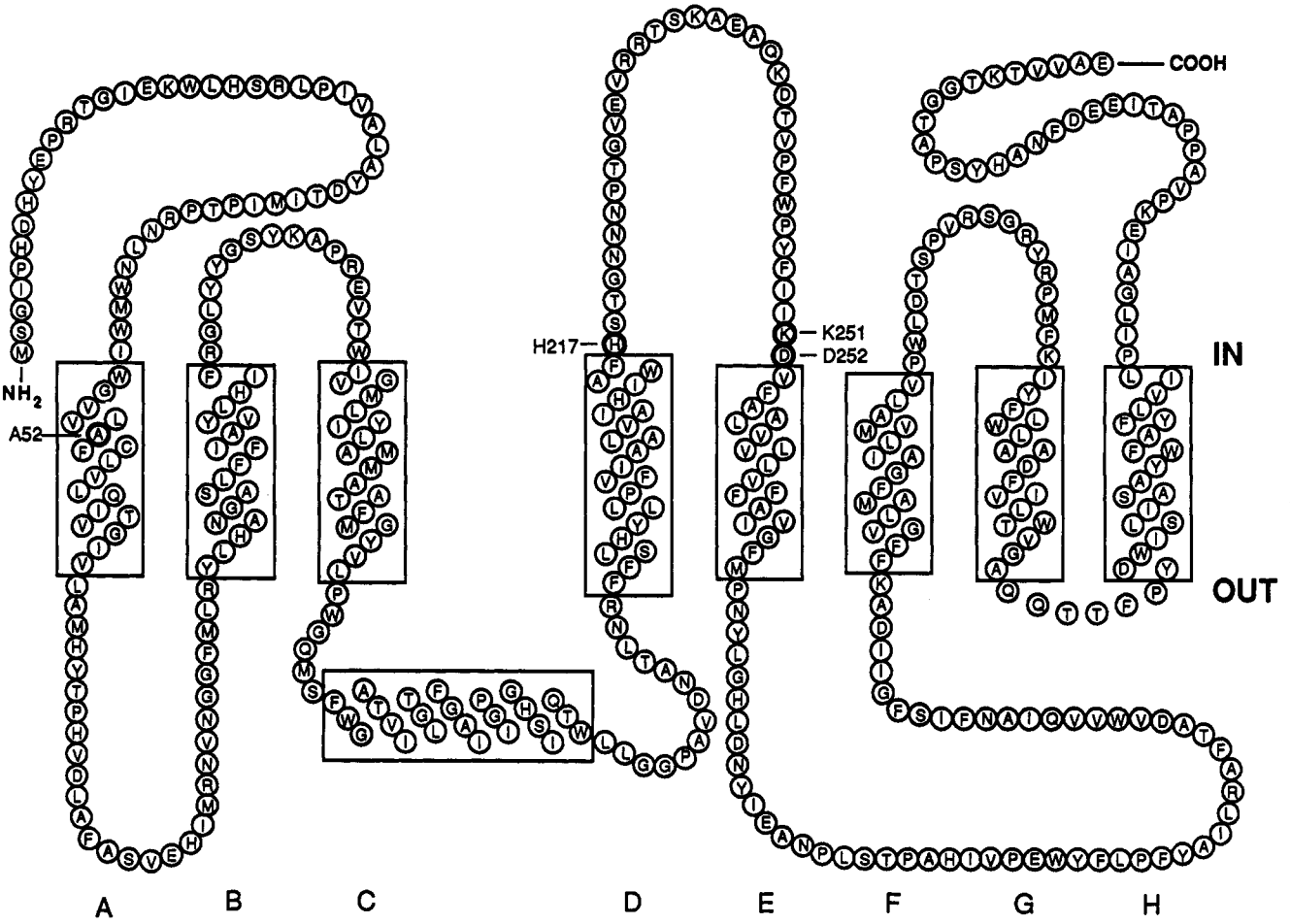

FIGURE 1: Model of the cytochrome *b* subunit of the bc_1 complex from *Rb. sphaeroides*. The amino acid residues altered by mutagenesis are indicated.

Table II: Summary of Some Characteristics of Strains of *Rb. sphaeroides* Containing Mutations in the Cytochrome *b* Subunit of the bc_1 Complex

strain	mutation	cytochrome b_L $E_{m,7}$ (mV)	cytochrome b_{H150} $E_{m,7}$ (mV)	cytochrome b_{H50} $E_{m,7}$ (mV)	[cytochrome b_H]/total[a] (μM)	cytochrome c_1 $E_{m,7}$ (mV)	photosynthetic growth
BC17C		-90	150	50	3.92	265	+++
Ga*b*K251I	K251I	-71	172	42	2.96	280	+++
Ga*b*K251M	K251M	-59	153	47	3.72	287	+++
Ga*b*D252N	D252N	-59	129	68	5.76	286	+++
Ga*b*D252A	D252A	-50	140	48	2.84	277	-----
Ga*b*H217A	H217A	-40	171	50	5.20	275	-----
Ga*b*A52V	A52V	-90	139	32	3.76	292	+++

[a] Amount of total cytochrome b_H in a suspension of chromatophores containing 8 mg/mL protein. This was determined by the sum of the species titrating near 50 mV (cytochrome b_{50}) and 150 mV (cytochrome b_{150}).

of the bc_1 complex was assayed by using difference spectra to measure the presence or absence of the cytochrome prosthetic groups. All of the mutants studied in this paper contained the normal complement of heme groups of the bc_1 complex, as determined by reduced-*minus*-oxidized spectra (spectra not shown). Some of the mutational changes cause shifts in the midpoint potentials of the cytochromes. Interestingly, the most dramatic shifts occur for cytochromes b_L and c_1 and not for cytochrome b_H, as expected. All of the mutants show an increase in the midpoint potential of cytochrome c_1 at pH 7.0 ($E_{m,7}$), and this was most marked in A52V. This influence of mutations in the cytochrome *b* subunit on the midpoint potential of cytochrome c_1 is unusual. With the exception of A52V, all of the mutants have midpoint potentials for cytochrome b_L which are higher than in the control strain, with H217A showing the largest (50 mV) increase in value. The other photosynthetically deficient mutant, D252A, also has an elevated $E_{m,7}$ for cytochrome b_L, although the effect is not as great as in H217A. Overall, there is no obvious pattern of change in the midpoint potential value with the residue change among the different strains. The data, however, indicate that these mutations result in subtle conformational changes that appear to have long-range effects.

Kinetics of Cytochrome b_H Reduction and Oxidation. The effects of the various mutations were further characterized by observing the changes in flash-induced kinetics of cytochrome b_H. Chromatophores are poised at 100 mV so that cytochromes b_L and b_H are almost totally oxidized before the flash, while the high-potential chain, consisting of cytochromes c_1 and c_2, the Rieske iron–sulfur center, and the reaction center are reduced. Inhibitors that block a specific electron pathway

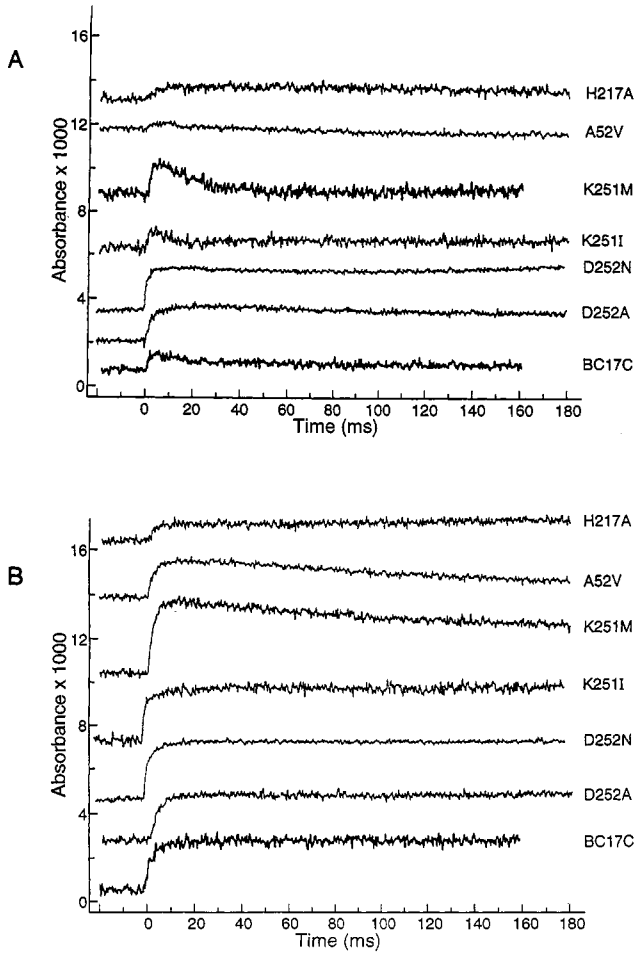

FIGURE 2: Flash-induced kinetics of cytochrome *b* for various mutants and the wild-type control (BC17C). Chromatophores were poised at 100 mV in a buffer containing 50 mM MOPS, pH 7.0, and 100 mM KCl. The figure shows the absorption difference between 561 and 569 nm. The data were obtained both in the absence (part A) of antimycin and in the presence of antimycin (part B).

within the bc_1 complex are then added to the sample. Turnover of the bc_1 complex is initiated by a >90% saturating flash of ~5-μs duration. The resulting changes in redox state are monitored using kinetic spectrophotometry on the millisecond time scale by selection of the appropriate wavelengths.

Figure 2 shows the flash-induced kinetic changes in the redox state of cytochrome b_H with and without antimycin present as an inhibitor of cytochrome b_H oxidation. In the BC17C strain with the wild-type *fbc* operon, cytochrome b_H shows a small transient reduction, followed by a slow reoxidation to the dark level observed prior to the flash. The small magnitude of the observed reduction of cytochrome b_H must result from a rapid initial reoxidation, prohibiting buildup of the reduced cytochrome. In the presence of antimycin, the reoxidation phase is inhibited, revealing the full extent and rate of cytochrome b_H reduction. Both K251I and K251M show behavior similar to that of the wild type (BC17C), except that the initial reoxidation rates in both strains must be considerably slower, resulting in an increased magnitude of the transient reduction. In strain A52V, the kinetics are similar to those of the wild-type control (BC17C). In the presence of antimycin, the extent of cytochrome b_H reduction in strains A52V and K251M reaches a maximal level, but then shows a slow reoxidation, even at high levels of inhibitor. In the other strains, antimycin induces a complete inhibition of cytochrome b_H reoxidation.

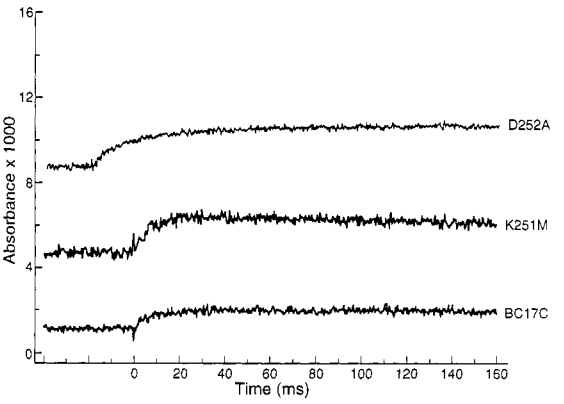

FIGURE 3: Flash-induced kinetics of cytochrome *b* for two mutants and the wild-type control (BC17C). Chromatophores were poised at 200 mV in the absence of antimycin. Shown is the absorption difference between 561 and 569 nm.

More interesting is the behavior of H217A, D252A, and D252N. The reduction of cytochrome b_H in the absence of antimycin shows kinetics similar to those of the wild type in the presence of antimycin. In these three mutants, the reoxidation of the cytochrome is blocked even in the absence of the inhibitor. In strains H217A, D252N, and D252A, the addition of antimycin causes little obvious change in the kinetics. However, with each of these three strains, and most noticeably in D252N, the addition of antimycin causes a small increase in the extent of cytochrome b_H reduction and a slight decrease in the rate of oxidation.

The kinetics were also measured at E_h 200 mV, where the bulk of the quinone pool is oxidized before the flash (Figure 3). In the wild-type control (BC17C), reduction of cytochrome b_H is slower than at E_h 100 mV (not shown), because at E_h 200 mV the equilibrium concentration of quinol is lower and the reduction of cytochrome b_H is limited by the amount of quinol produced photochemically. In the absence of antimycin at E_h 200 mV (Figure 3), a partial reduction of cytochrome b_H is seen, but, despite the oxidized state of the quinone pool, the cytochrome does not become completely reoxidized. The fraction of cytochrome which remains reduced, even 100 ms after the flash, is equivalent to ~25–30% of the cytochrome b_H reduced in the presence of antimycin. Complete reoxidation of cytochrome b_H is not seen at E_h values above 130 mV. Although this behavior is not well understood, it most likely reflects the equilibration at the Q_c-site between reduced cytochrome b_H, bound semiquinone ($Q^{\bullet-}$), and the quinone pool. This same set of reactions is probably involved in the formation of the higher potential form of cytochrome b_H, cytochrome b_{150} (de la Rosa & Palmer, 1983; Meinhardt & Crofts, 1983; Rich et al., 1989; Salerno et al., 1989).

In several of the mutant strains, this paradoxical redox behavior is amplified (Figure 3). In strain K251M, the fraction of cytochrome b_H remaining reduced 100 ms after flash-activation of chromatophores poised at E_h 200 mV is equal to the cytochrome reduced in the presence of antimycin at the same E_h, and is ~60% of the total cytochrome reduced in the presence of antimycin at E_h 100 mV. In strain D252A (Figure 3), the extent of stably reduced cytochrome b_H is even higher. In each case, the oxidation phase of cytochrome b_H, at the inhibited rate, is only observed at E_h values lower than 130 mV. This behavior is discussed below in the context of the antimycin-induced oxidation of cytochrome b_{150}.

Electrogenic Reactions Associated with Cytochrome b_H Oxidation. The turnover of the bc_1 complex in chromatophores can also be monitored by measurement of the electrogenic

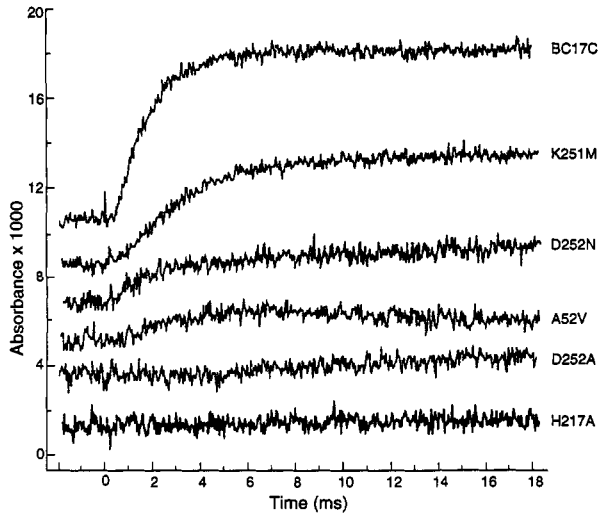

FIGURE 4: Kinetics of the electrochromic absorption changes following flash illumination. The traces show the slow phase at 503 nm following a single flash. The antimycin-sensitive portion of the slow phase is obtained by subtracting the carotenoid absorption change in the presence of antimycin from an absorption change observed without inhibitors.

processes. It has been shown that the development of a membrane potential as a consequence of electrogenic processes can be followed by assaying absorption changes due to the electrochromic bandshifts of carotenoids measured at 503 nm (Jackson & Crofts, 1971). The slow phase of the carotenoid absorption change is associated with electrogenic processes in the bc_1 complex (Glaser & Crofts, 1984). When the sample is poised at E_h 100 mV, the rate and extent of the slow phase are close to maximal. The addition of antimycin inhibits a large portion of the slow phase. This antimycin-sensitive component of the carotenoid change reflects the oxidation of cytochrome b_H, and is due to the electrogenic processes accompanying oxidation of the cytochrome, as well as the second turnover of the bc_1 complex which can occur when an electron leaves the b-cytochrome chain (Crofts et al., 1983; Glaser & Crofts, 1984). The traces in Figure 4 show the antimycin-sensitive component of the carotenoid change obtained by subtraction of the kinetic traces of the change without or with antimycin. Each of the mutants has a reduced rate of the antimycin-sensitive carotenoid change as compared to the wild-type control (BC17C), suggesting an impaired oxidation of cytochrome b_H. Strains K251I and K251M show a change of similar magnitude to that of BC17C, but with a reduced rate (K251I kinetics not shown). A52V and D252N have rates more severely inhibited compared to BC17C, as well as a smaller amplitude compared to that of the wild type. In mutants D252A and H217A, the electron transfer from cytochrome b_H is so strongly inhibited that no antimycin-sensitive carotenoid change is seen during the relatively short time span of the kinetic trace.

The reduction of cytochrome b_H is also electrogenic, and this can be measured through the myxothiazol-sensitive component of the carotenoid bandshift observed in the presence of antimycin. All strains show kinetics for this component of the electrogenic process similar to those of the wild-type BC17C strain (not shown). These results are in good agreement with the results from flash-induced kinetics of cytochrome b_H redox changes, which show that the inhibition of electron flow in the mutant strains is localized at the step of cytochrome b_H oxidation. The inhibition is most severe in strains D252A and H217A, which fail to grow photosynthetically, is quite marked in strains D252N and A52V, and is relatively mild in strains K251M and K251I. All strains which show a significant rate of turnover of the bc_1 complex, as judged by the antimycin-sensitive carotenoid absorption change, are able to grow photosynthetically.

Antimycin Binding in Mutant Strains. Antimycin inhibits the function of the bc_1 complex by blocking electron flow from cytochrome b_H to the quinone reducing (Q_c) site (Crofts et al., 1983; Mitchell, 1976). The exact mechanism of antimycin inhibition if not known, but it is likely that antimycin binds at the Q_c-site and blocks access of quinone to the site. The effect that the mutations have on the binding of antimycin can be measured through flash-induced kinetics. Aliquots of antimycin are added to samples of each strain poised at E_h 100 mV, and the flash-induced absorption changes of cytochrome b_H are monitored at the appropriate wavelengths. Figure 5 shows the effect of antimycin titration on the extent of cytochrome b_H reduction measured 10 ms after the flash for each mutant. The data have been normalized to account for the differing total amounts of cytochrome b_H that each mutant produces (Table II). The plots show that all of the mutants bind antimycin, but several strains show a somewhat weaker binding of antimycin than does the wild type (BC17C), on the basis of the observation that a relatively larger amount of antimycin is required to reach saturation. Using this qualitative criterion, strains A52V and K251M show the weakest antimycin binding. The equivalent mutations in yeast have been found to be antimycin–resistant. Some strains that show a strongly inhibited rate of reoxidation of cytochrome b_H (e.g., D252N) bind antimycin as well or nearly as well as does the wild type. It is interesting to note that there is no major difference between the antimycin binding titer for the nonphotosynthetic mutants, H217A and D252A, and the other photosynthetically competent mutants.

Antimycin Binding Assayed through Antimycin-Induced Oxidation of Cytochrome b_{150}. Redox titrations of cytochrome b in chromatophores show a component which titrates with an $E_{m,7}$ of about 150 mV. In the presence of antimycin, a fraction of this component is converted to a form which titrates at $E_{m,7}$ about 50 mV, and is indistinguishable from cytochrome b_H, the major component titrating in this range. It has been speculated (de la Rosa & Palmer, 1983; Meinhardt & Crofts, 1983; Rich et al., 1989; Salerno et al., 1989) that cytochrome b_{150} is a form of cytochrome b_H in complexes with a semiquinone bound at the Q_c-site (i.e., $b_{150}Q^{\bullet-}$). These forms are included in the schematic in Figure 7. If chromatophores are poised at E_h 110 mV, the addition of antimycin induces an oxidation of cytochrome b, indicating the conversion of cytochrome b_{150}, which is predominantly reduced at this potential, to cytochrome b_H (i.e., cytochrome b_{50}), which is predominantly oxidized at this potential (Meinhardt & Crofts, 1983). This is rationalized by the displacement by antimycin of all species of quinone (Q, $Q^{\bullet-}$, and QH_2) at the Q_c-site (see Figure 7).

One method for measuring antimycin binding is to quantify the titer for antimycin-induced oxidation of cytochrome b_{150}. Figure 6 shows titrations of the antimycin-induced oxidation for the strains studied, normalized to the total cytochrome b_H seen in dark redox titrations, i.e., the sum of cytochromes b_{50} and b_{150}. This normalization procedure is necessary to allow comparison between strains with different levels of expression of the cytochrome bc_1 complex. The end point of each titration is a good indicator of how well the mutants bind antimycin. All mutants show an antimycin-induced oxidation of cytochrome b_{150}, with a relatively strong binding of antimycin.

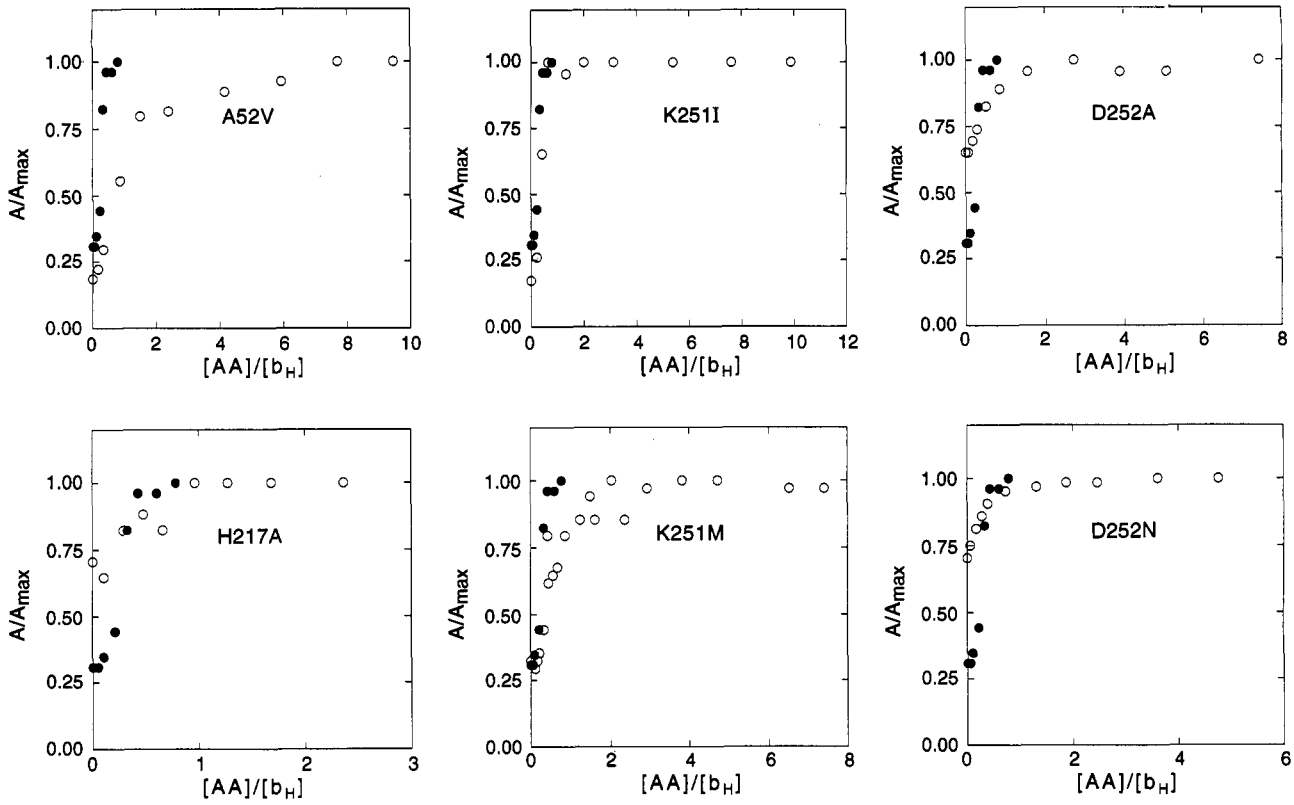

FIGURE 5: Binding of antimycin monitored using flash-induced kinetic data. Samples were poised at 100 mV before aliquots of antimycin were added. The absorbance changes observed and the antimycin concentrations were normalized for each mutant with respect to cytochrome b_H to allow for comparison. The solid circles (●) represent the wild-type BC17C sample.

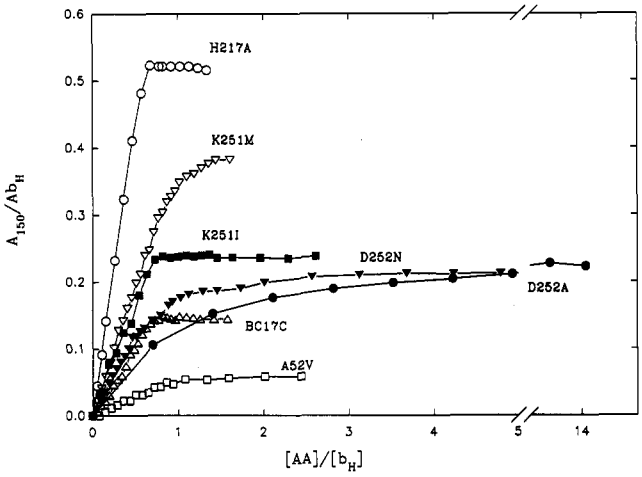

FIGURE 6: Antimycin-induced oxidation of cytochrome b_{150}. Samples were poised at 100 mV. The absorbance change due to the oxidation of cytochrome b_{150} (A_{150}) is normalized by the total absorbance change expected (Ab_H) is all of the cytochrome b_H were in the high-potential (b_{150}) form. The amount of antimycin (AA) added is also normalized by the total amount of cytochrome b_H which is present in the chromatophores. Details are present in the text.

Strains H217A and K251I show end points for the titration which are, within experimental error, the same as for the wild-type BC17C strain, and all three strains show the sharp end point characteristic of a tightly binding inhibitor. Strains K251M, A52V, D252N, and D252A show weaker binding, as indicated both by the higher titer and by the curvature of the approach to the end point of the titration. The most marked difference between strains is in the amplitude of the antimycin-induced oxidation. This is most dramatic in H217A, where more than half of the total cytochrome b_H titrates as b_{150}, and becomes oxidized on addition of antimycin. However, all mutant strains apart from A52V show an enhanced antimycin-induced oxidation when compared to that of the wild-type strain.

Interpretation of these results depends on an understanding of the mechanism of quinone reduction at the Q_c-site, and this is at present very incomplete. It has been proposed that the antimycin-induced oxidation of cytochrome b_{150} involves a displacement of the equilibria at the Q_c-site summarized in Figure 7, where b_H represents the Q_c-site with associated cytochrome b_H. This cytochrome has an $E_{m,7}$ of 50 mV (denote b_H in Figure 7) except when a semiquinone species ($Q^{\bullet-}$) is bound at the Q_c-site, when it has $E_{m,7}$ of 150 mV (denoted (b_{150} in Figure 7).

Figure 7 illustrates the partial reactions in the turnover of the two-electron gate thought to operate at the Q_c-site. The two-electron reduced state of the low-potential chain of the complex (VII in Figure 7) can be reached either by reduction of the oxidized complex following binding of quinol at the Q_c-site (I → VIII → VII) or by electron transfer into the *b*-cytochrome chain following oxidation of $2QH_2$ at the Q_z-site (II → III → IV → VI → VII).

In the context of this mechanism, the antimycin-induced oxidation of cytochrome b_{150} occurs when antimycin is added to the complex in the two-electron reduced state (VI, VII, and VIII) and reflects that fraction of complexes in which an electron resides initially on both cytochrome b_{150} and $Q^{\bullet-}$ (species VII). The greater amplitude of the change in some strains would then indicate a greater stability of this state (VII), relative to VIII. This would also be a reasonable explanation for the severely impaired rate of electron transfer from cytochrome b_H to the Q_c-site (VII → VIII and/or IV → V) that is observed with some of the mutants. Enhanced stability of VII could also correlate with the apparent weakness

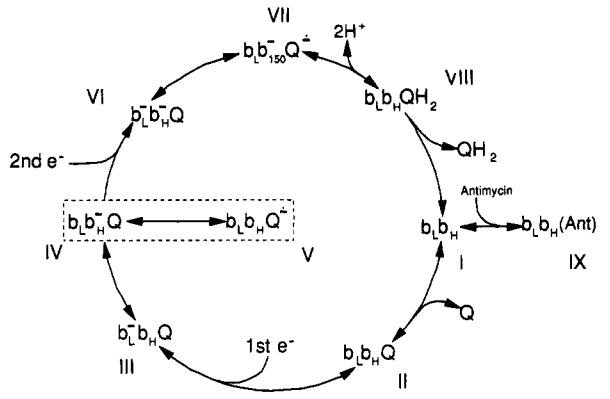

FIGURE 7: Schematic of the proposed states of the low-potential branch of the bc_1 complex. Cytochrome b_L is denoted simply as b_L, and is at the quinol oxidizing (Q_z) site. The Q_c-site, or quinol reductase site, is symbolized by b_H, representing cytochrome b_H. This site can accommodate quinone (Q), quinol (QH_2), or semiquinone ($Q^{\bullet-}$), as well as antimycin (Ant). When a semiquinone species is bound to the Q_c-site, it is proposed that the apparent $E_{m,7}$ of the high-potential cytochrome at this site (b_H) increases from 50 to 150 mV. The notation of b_H in this state is changed to b_{150}. Turnovers at the Q_z site are induced by light flashes, producing in a concerted mechanism the first and the second electron to enter this branch of the bc_1 complex, as indicated in the figure. The relative stability of each of the species shown in this figure when chromatophores are poised at different E_h values is discussed in the text.

of antimycin binding, since presumably antimycin and quinone compete for binding to the same site.

The presence of stably reduced cytochrome *b* following flash activation when the quinone pool is primarily oxidized (see Figure 3) can also be discussed in the context of the scheme in Figure 7. The effect could reflect complexes with the low-potential chain reduced by either one or two electrons. In the former case, it would be necessary to postulate that the electron-transfer step IV → V is unfavorable, suggesting a low E_m for the $Q/Q^{\bullet-}$ couple at the Q_c-site, corresponding to an unstable bound semiquinone. Such an explanation has been suggested for the similar phenomenon observed in the b_6f complex of chloroplasts (Kramer & Crofts, 1992), but it seems unlikely that this is the case in the chromatophore complex, because many studies have shown the presence of a relatively stable semiquinone at the Q_c-site (de la Rosa & Palmer, 1983; McCurley et al., 1990; Meinhardt & Ohnishi, 1992; Salerno et al., 1989). The alternative, that the stable reduction reflects complexes with two electrons in the low-potential chain, would imply both that a substantial fraction of complexes reaches this state and that the electron-transfer step VII → VIII is unfavorable. This would suggest a low potential for the $Q^{\bullet-}/QH_2$ couple, i.e., a stable semiquinone. This would be compatible with the correlation between enhanced antimycin-induced oxidation of cytochrome b_H and a greater extent of stably reduced cytochrome b_H following flash activation with the quinone pool oxidized, observed in the set of mutants studied here. However, the formation of the two-electron reduced state of the low-potential chain (VI, VII, and VIII) would require either that the light flash causes double turnovers of the Q_z-site in a substantial fraction of complexes or that there is a predominant partitioning of the QH_2 produced photochemically to the Q_c-site (i.e., VIII is favored over I and II). Further studies of these strains, in which the probability of double turnovers of the Q_z-site is varied by varying the flash intensity, will throw further light on this question. EPR spectroscopy will also be used to investigate more directly the stability of the semiquinone at the Q_c-site.

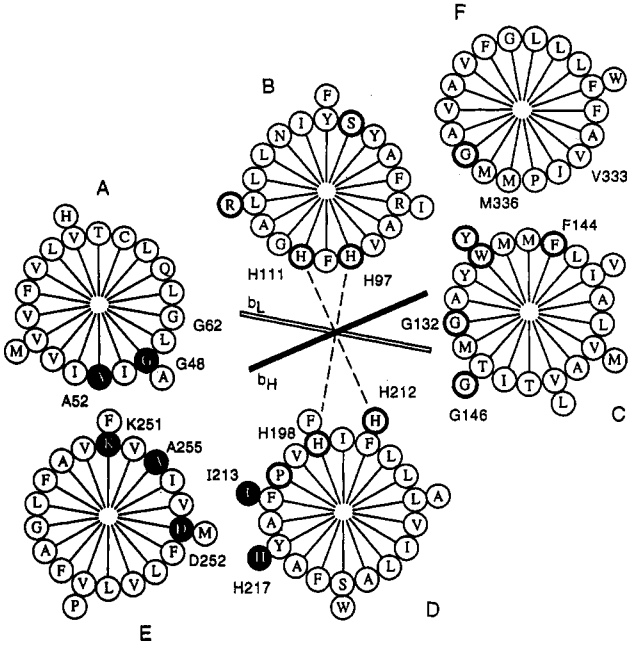

FIGURE 8: Helical wheel diagram showing a likely arrangement of six out of the eight transmembrane helices of the cytochrome *b* subunit as viewed from the cytoplasmic side of the chromatophore membrane. The two hemes are shown edge-on-ligated to the histidines located in helix B and helix D. Residues postulated to be at the Q_c-site are shown as filled circles (see text), and other very highly conserved residues are indicated by a thick ring. The boundaries of several helices are extended beyond those shown in Figure 1 in order to show the putative positions of important hydrophilic residues, most notably H217, K251, and D252.

Structure/Function Relationships. The analysis of cytochrome b_H oxidation–reduction kinetics and the electrogenic processes associated with these electron-transfer reactions show clearly that the mutations studied in this paper have their main effect on the oxidation of cytochrome b_H. This finding provides some confidence in the structural model which identifies these residues as close to the putative Q_c-site (antimycin binding site). The locations of the residues discussed in this work, together with others whose modification gives rise to inhibitor resistance at the Q_c-site, are shown in the two-dimensional helical cylinder model of Figure 8. The arrangement of the helices in the membrane plane must allow these residues to occupy a common volume defining the catalytic (antimycin binding) site. The helical wheel model in Figure 8 represents a view from the cytoplasmic side of the membrane showing a possible arrangement of six of the helices for which structurally pertinant information is available (Crofts et al., 1992). Helices B and D contain the ligands to cytochrome b_L (His97 and His198) and cytochrome b_H (His111 and His212). Helices A and C are placed in the model so that the pairs of totally conserved glycines, Gly48/Gly62 (helix A) and Gly132/Gly146 (helix D), can facilitate the packing of the two hemes. Those residues that have been identified by mutants that influence Q_c-site function or inhibitor binding occupy a defined volume on the cytoplasmic side of the cytochrome *b* subunit in this model (Crofts et al., 1992). These include the following: (i) Ala52 and Lys251, where mutational changes weaken antimycin binding (Figure 5); (ii) His217 and Asp252, where mutational changes block Q_c-site function (Figure 1). These are suitably positioned in the model to form a salt-bridge, which could be tested by additional mutagenesis experiments. Alternatively, Asp252 and Lys251 could form a salt-bridge. (iii) Gly48 is the site

where a mutational change inhibits Q_c-site function (Yun et al., 1992). (iv) Ala255 (equivalent to yeast Gly231) is the site of an HQNO-resistant mutant in mouse (Howell et al., 1987). (v) Ile213 is the site of a funiculosin-resistant mutant in yeast (diRago et al., 1990).

In addition to the residues in putative helices, lesions conferring resistance to inhibitors at the Q_c-site are found at several other locations in the sequence. The span to the N-terminal side of I33, equivalent to the residue modified in the mutation I17F in yeast, which confers diuron resistance (Tsai et al., 1985), contains a section showing conserved amphipathy at the helical repeat, suggesting a helical configuration in the folded protein. It is possible that this region (helix a) forms a helical "cap" to a quinone binding pocket defined by membrane helices A, D, and E. This would give a structure similar to that of the two-electron gate of the bacterial reaction centers.

CONCLUSIONS

Mutations have been made in residues that are predicted to be on the cytoplasmic side of the cytochrome *b* subunit of the bc_1 complex. The four targets for mutagenesis are either coincident with or nearby residues where missense mutations are known to confer resistance to inhibitors of the quinone reductase Q_c-site. All of the mutants have a slow rate of electron transfer from cytochrome b_H to the Q_c-site. These results support the assumption that the loci of inhibitor-resistance mutants define a structural and functional domain within the cytochrome *b* subunit that is the Q_c-site. It cannot be concluded that any of the four residues examined in this work is absolutely essential for Q_c-site function.

In addition to having an impaired rate of reoxidation of cytochrome b_H, each of the mutants has an increased proportion of the total cytochrome b_H in the form of cytochrome b_{150}. These data generally support the idea that the phenotype of the mutants results from an altered stability of a semiquinone intermediate at the Q_c-site.

Several mutants were obtained with very severe defects in Q_c-site function, yet are able to grow photosynthetically. Even a marginally active bc_1 complex can support photosynthetic growth under the conditions employed.

ACKNOWLEDGMENT

We thank Dr. Chang-Hyon Yun for advice and assistance in the initiation of this project.

REFERENCES

Atta-Asafo-Adjei, E., & Daldal, F. (1991) *Proc. Natl. Acad. Sci. U.S.A. 88*, 492–496.
Bacious, L., Sinning, I., & Sebban, P. (1991) *Biochemistry 30*, 9110–9116.
Bowyer, J. R., Tierney, G. V., & Crofts, A. R. (1979) *FEBS Lett. 101*, 201–206.
Crofts, A. R. (1985) in *The Mechanism of the Ubiquinol: Cytochrome c Oxidoreductases of Mitochondria and of Rhodopseudomonas sphaeroides* (Martonosi, A. N., Ed.) pp 347–382, Plenum Publishing Corp., New York.
Crofts, A. R., & Wang, Z. (1989) *Photosynth. Res. 22*, 69–87.
Crofts, A. R., Meinhardt, S. W., Jones, K. R., & Snozzi, M. (1983) *Biochim. Biophys. Acta 723*, 202–218.
Crofts, A., Hacker, B., Barquera, B., Yun, C.-H., & Gennis, R. (1992) *Biochim. Biophys. Acta 1101*, 162–165.
Daldal, F., Tokito, M. K., Davidson, E., & Faham, M. (1989) *EMBO J. 8*, 3951–3961.
de la Rosa, F. F., & Palmer, G. (1983) *FEBS Lett 163*, 140–143.
Ding, H., Robertson, D. E., Daldal, F., & Dutton, P. L. (1992) *Biochemistry 31*, 3144–3158.
diRago, J.-P., & Colson, A.-M. (1988) *J. Biol. Chem. 263*, 12564–12570.
diRago, J.-P., Perea, X., & Colson, A.-M. (1986) *FEBS LEtt. 208*, 208–210.
diRago, J.-P., Coppée, J.-Y., & Colson, A.-M. (1989) *J. Biol. Chem. 264*, 14543–14548.
diRago, J.-P., Perea, J., & Colson, A.-M. (1990) *FEBS Lett. 263*, 93–98.
Dutton, P. L. (1978) *Methods Enzymol. 54*, 411–435.
Gabellini, N. (1988) *J. Bioenerg. Biomembr. 20*, 59–83.
Glaser, E. G., & Crofts, A. R. (1984) *Biochim. Biophys. Acta 766*, 322–333.
Hauska, G., Nitschke, W., & Herrmann, R. G. (1988) *J. Bioenerg. Biomembr. 20*, 211–228.
Howell, N., & Gilbert, K. (1988) *J. Mol. Biol. 203*, 607–618.
Howell, N., Appel, J., Cook, J. P., Howell, B., & Hauswirth, W. W. (1987) *J. Biol. Chem. 262*, 2411–2414.
Jackson, J. B., & Crofts, A. R. (1971) *Eur. J. Biochem. 18*, 120–130.
Kiley, P. J., & Kaplan, S. (1988) *Microbiol. Rev. 52*, 50–69.
Leuking, D. R., Fraley, R. T., & Kaplan, S. (1978) *J. Biol. Chem. 253*, 451–457.
McCurley, J. P., Miki, T., Yu, L., & Yu, C.-A. (1990) *Biochim. Biophys. Acta 1020*, 176–186.
Meinhardt, S. W., & Crofts, A. R. (1983) *Biochim. Biophys. Acta 723*, 219–230.
Meinhardt, S. W., & Ohnishi, T. (1992) *Biochim. Biophys. Acta 1100*, 67–74.
Mitchell, P. (1976) *J. Theor. Biol. 62*, 327–367.
Rich, P. R., Jeal, A. E., Madgwick, S. A., & Moody, A. J. (1989) *Biochim. Biophys. Acta 1018*, 29–40.
Robertson, D. E., Daldal, F., & Dutton, P. L. (1990) *Biochemistry 29*, 11249–11260.
Salerno, J. C., Xu, Y., Osgood, M. P., Kim, C. H., & King, T. E. (1989) *J. Biol. Chem. 264*, 15398–15403.
Sambrook, J., Fritsch, E. F., & Maniatis, T. (1989) in *Molecular Cloning: A Laboratory Manual*, Cold Spring Harbor Laboratory, Cold Spring Harbor, NY.
Sinning, I., Michel, H., Mathis, P., & Rutherford, A. W. (1989) *Biochemistry 28*, 5544–5553.
Trumpower, B. L. (1990a) *Microbiol. Rev. 54*, 101–129.
Trumpower, B. L. (1990b) *J. Biol. Chem. 265*, 11409–11412.
Tsai, A.-L., Kauten, R., & Palmer, G. (1985) *Biochim. Biophys. Acta 806*, 418–426.
Vandeyar, M. A., Weiner, M. P., Hutton, C. J., & Batt, C. A. (1988) *Gene 65*, 129–133.
Vieira, J., & Messing, J. (1982) *Gene 19*, 259–268.
Weber, S., & Wolf, K. (1988) *FEBS Lett. 237*, 31–34.
Yun, C.-H., Beci, R., Crofts, A. R., Kaplan, S., & Gennis, R. B. (1990) *Eur. J. Biochem. 194*, 399–411.
Yun, C.-H., Crofts, A. R., & Gennis, R. B. (1991a) *Biochemistry 30*, 6747–6754.
Yun, C.-H., Van Doren, S. R., Crofts, A. R., & Gennis, R. B. (1991b) *J. Biol. Chem. 266*, 10967–10973.
Yun, C.-H., Wang, Z., Crofts, A. R., & Gennis, R. B. (1992) *J. Biol. Chem. 267*, 5901–5909.